

# X-ray Structure Determinations of Li[CF<sub>3</sub>SO<sub>2</sub>N(CH<sub>2</sub>)<sub>3</sub>OCH<sub>3</sub>] and the Solid Electrolyte [LiC12-C-4][CF<sub>3</sub>SO<sub>2</sub>N(CH<sub>2</sub>)<sub>3</sub>OCH<sub>3</sub>]

Rensl E. A. Dillon, Charlotte L. Stern, and Duward F. Shriver\*

Department of Chemistry and Materials Research Center, Northwestern University,  
Evanston, Illinois 60208-3113

Received December 6, 1999. Revised Manuscript Received February 2, 2000

The crystal structures of the lithium salt, Li[CF<sub>3</sub>SO<sub>2</sub>N(CH<sub>2</sub>)<sub>3</sub>OCH<sub>3</sub>] and its 12-C-4 complex [LiC12-C-4][CF<sub>3</sub>SO<sub>2</sub>N(CH<sub>2</sub>)<sub>3</sub>OCH<sub>3</sub>] demonstrate a change in the lithium coordination environment upon complex formation. The longer Li–N bond distance in [LiC12-C-4][CF<sub>3</sub>SO<sub>2</sub>N(CH<sub>2</sub>)<sub>3</sub>OCH<sub>3</sub>] indicates that the 12-C-4 crown ether weakens the interactions between the lithium cation and the [CF<sub>3</sub>SO<sub>2</sub>N(CH<sub>2</sub>)<sub>3</sub>OCH<sub>3</sub>]<sup>−</sup> anion. Correlations between these structures and previously reported vibrational spectroscopy and ionic conductivity are presented.

## Introduction

Major issues in the field of ion-conducting polymer electrolytes include the local structural arrangements of the polymer and salt and their role in ion transport.<sup>1–4</sup> The low dielectric constants of the polymer hosts typically used in polymer electrolytes, resulting in the formation of ion pairs or higher aggregates, has a strong and often detrimental influence on ionic conductivity. Raman and infrared spectroscopy are useful tools to detect and explore ion pairing;<sup>5,6</sup> however, vibrational spectroscopy does not provide information on the exact positions of the atoms, such as the detailed coordination environment of the cation. Single X-ray diffraction provides more precise information for crystalline materials, but as shown by Berthier and others, ion transport primarily occurs in the amorphous region of the polymer electrolyte.<sup>7</sup> The combination of information from vibrational spectroscopy and single-crystal X-ray diffraction provides a valuable approach to the understanding of polymer–salt interactions in both the crystalline and amorphous phases. This information suggests strategies for improving ion transport. For example, X-ray diffraction data show that the lithium cation in (PEO)<sub>3</sub>:LiCF<sub>3</sub>SO<sub>3</sub> is coordinated to five oxygens: three ether oxygens and one sulfonyl oxygen from each of two different CF<sub>3</sub>SO<sub>3</sub><sup>−</sup> anions.<sup>8,9</sup> The structure indicates little interchain interaction and the helical conformation of the polymer results in a columnar

coordination complex. Similarly, the crystal structure of (PEO)<sub>3</sub>:Li[(CF<sub>3</sub>SO<sub>2</sub>)<sub>2</sub>N] shows that lithium is coordinated by three ether oxygens from the polymer chain and one sulfonyl oxygen from each of two different [(CF<sub>3</sub>SO<sub>2</sub>)<sub>2</sub>N]<sup>−</sup>.<sup>10</sup> The major difference between these structures is that the larger [(CF<sub>3</sub>SO<sub>2</sub>)<sub>2</sub>N]<sup>−</sup> forces the polymer chains apart, and hinders their ability to pack efficiently. This observation along with the flexible configuration and, delocalized negative charge on the [(CF<sub>3</sub>SO<sub>2</sub>)<sub>2</sub>N]<sup>−</sup> anion may account for the low melting point and high conductivity of the (PEO)<sub>3</sub>:Li[(CF<sub>3</sub>SO<sub>2</sub>)<sub>2</sub>N] complex. Before the crystal structures of these complexes were obtained, vibrational spectroscopy indicated similar lithium coordination environments for both complexes.<sup>8</sup>

In a previous paper, we explored the use of cation-coordinating macrocycles to form amorphous electrolytes.<sup>11</sup> These macrocycles surround the cation and thereby reduce the Coulombic interaction between the cation and anion. We found that a match between the cation radius and that of the macrocycle cavity results in a crystalline complex with a low melting temperature and relatively low conductivity. However, when the cavity of the macrocycle is larger than that of the cation the resulting complex is a glass which has a subambient glass transition temperature and high ionic conductivity. In the present work crystal structures were determined for the salt, Li[CF<sub>3</sub>SO<sub>2</sub>N(CH<sub>2</sub>)<sub>3</sub>OCH<sub>3</sub>] and [LiC12-C-4][CF<sub>3</sub>SO<sub>2</sub>N(CH<sub>2</sub>)<sub>3</sub>OCH<sub>3</sub>]. The latter structure verifies the encapsulation of the lithium cation by the crown ether, and it helps to explain the formation of amorphous phases for systems in which there is a mismatch between the crown cavity and the ion radius. The structures also support the interpretation of vibrational spectra described elsewhere.<sup>12</sup>

(1) Gray, F. M. *Solid Polymer Electrolytes: Fundamentals and Technological Applications*; VCH Publishers: New York, 1991.

(2) *Polymer Electrolyte Reviews 1*; MacCallum, J. R., Vincent, C. A., Eds.; Elsevier Science Publishers LTD: London, 1987.

(3) Ratner, M. A.; Shriver, D. F. *Chem. Rev.* **1988**, *88*, 109.

(4) Armand, M. *Solid State Ionics* **1994**, *69*, 309.

(5) Papke, B. L.; Ratner, M. A.; Shriver, D. F. *J. Phys. Chem. Solids* **1981**, *42*, 493.

(6) Papke, B. L.; Ratner, M. A.; Shriver, D. F. *J. Electrochem. Soc.* **1982**, *129*, 1434.

(7) Berthier, C.; Gorecki, W.; Minier, M.; Armand, M. B.; Chabagno, J. M.; Rigaud, P. *Solid State Ionics* **1983**, *11*, 91.

(8) Lightfoot, P.; Mehta, M. A.; Bruce, P. G. *Science* **1993**, *262*, 883.

(9) Andreev, Y. G.; Lightfoot, P.; Bruce, P. G. *Chem. Commun.* **1996**, 2169.

(10) Andreev, Y. G.; Lightfoot, P.; Bruce, P. G. *J. Appl. Crystallogr.* **1997**, *18*, 294.

(11) Dillon, R. E.; Shriver, D. F. In *Materials Research Society*; Ginley, D. S., Doughty, D. H., Scrosati, B., Takamura, T., Zhang, Z., Eds.; Materials Research Society: Boston, 1998; Vol. 496.

(12) Dillon, R. E. A.; Shriver, D. F. *Chem. Mater.* **1999**, *11*, 3296–3301.

**Table 1. Crystallographic Data**

	$(\text{Li}[\text{CF}_3\text{SO}_2\text{N}(\text{CH}_2)_3\text{OCH}_3])_2 \cdot \text{CH}_3\text{CN}$	$[\text{LiC}12\text{-C-4}][\text{CF}_3\text{SO}_2\text{N}(\text{CH}_2)_3\text{OCH}_3]$
empirical formula	$\text{C}_{12}\text{H}_{21}\text{F}_6\text{N}_3\text{O}_6\text{Li}_2\text{S}_2$	$\text{C}_{13}\text{LiNO}_7\text{H}_{25}\text{F}_3\text{S}$
formula weight	495.31	403.34
crystal color, habit	colorless, needle	colorless, block
crystal dimensions, mm	$0.40 \times 0.16 \times 0.10$	$0.42 \times 0.41 \times 0.29$
crystal system	monoclinic	monoclinic
space group	$P2_1/c$ (no. 14)	$P2_1/c$ (no. 14)
lattice type	primitive	primitive
lattice parameters:		
$a$ , Å	10.8090(8)	8.9357(5)
$b$ , Å	20.5005(2)	14.4103(8)
$c$ , Å	10.2385(8)	14.2559(8)
$\beta$ , Å	95.721(2)	90.6990(10)
$V$ , Å <sup>3</sup>	2257.9(3)	1835.5(2)
$Z$ value	4	4
$D_{\text{cacl}}$ , g cm <sup>-3</sup>	1.457	1.459
$F000$	1016.00	848.00
$\mu$ (Mo K $\alpha$ ), cm <sup>-1</sup>	3.16	2.40
$T$ , °C	-120	-120
$R_1^a$	0.039	0.032
$wR_2^b$	0.075	0.060
goodness of fit	1.63	2.82

## Experimental Section

**Materials.** All experimental manipulations were carried out under an inert atmosphere of dry nitrogen.  $\text{Li}[\text{CF}_3\text{SO}_2\text{N}(\text{CH}_2)_3\text{OCH}_3]$  was prepared as previously described.<sup>13</sup> 12-C-4 (1,4,7,10-tetraoxacyclododecane) was purchased from Aldrich and dried over molecular sieves for more than 48 h. Tetrahydrofuran (THF) was distilled under nitrogen from sodium benzophenone. An equimolar ratio of  $\text{Li}[\text{CF}_3\text{SO}_2\text{N}(\text{CH}_2)_3\text{OCH}_3]$  and 12-C-4 was dissolved in THF and the solvent was removed under a vacuum at 50 °C ( $1 \times 10^{-1}$  Torr), followed by 40 °C ( $8 \times 10^{-6}$  Torr). Samples were shown to be free of residual solvent and water by infrared spectroscopy.

**X-ray Crystal Structure of  $(\text{Li}[\text{CF}_3\text{SO}_2\text{N}(\text{CH}_2)_3\text{OCH}_3])_2 \cdot \text{CH}_3\text{CN}$  (I).** A colorless needle crystal of  $\text{Li}[\text{CF}_3\text{SO}_2\text{N}(\text{CH}_2)_3\text{OCH}_3]$  was grown by slow diffusion of methylene chloride into a solution of the salt in acetonitrile. A crystal with dimensions of  $0.40 \times 0.16 \times 0.10$  mm was mounted using oil (Paratone-N, Exxon) on a glass fiber and transferred to a Bruker Smart 1000 diffractometer. All measurements were made on a CCD plate area detector with graphite monochromated Mo-K $\alpha$  radiation. Cell constants and an orientation matrix for data collection corresponded to a primitive monoclinic cell. A summary of the crystallographic data is given in Table 1. The dimensions of the cell yield a calculated density of  $1.46 \text{ g cm}^{-3}$  ( $Z = 4$  and  $\text{FW} = 495.31$ ) and the systematic absences of  $h0l$ :  $l \pm 2n$  and  $0k0$ :  $k \pm 2n$  uniquely determine the space group to be  $P2_1/c$  (no. 14). The data were collected at a temperature of  $-120 \pm 1$  °C to a maximum  $2\theta$  value of  $56.5^\circ$ , in  $0.30^\circ$  oscillations with 30.0 s exposures. The crystal to detector distance was 50.23 mm. The detector swing angle was  $28.00^\circ$ .

Of the 16 435 reflections collected, 5452 were unique ( $R_{\text{int}} = 0.043$ ). Data were collected and processed using the SMART (NT) and SAINT (NT) program from Bruker. A linear absorption coefficient,  $\mu$ ,  $3.2 \text{ cm}^{-1}$ , for Mo K $\alpha$  radiation was used. The data were corrected for Lorentz and polarization effects. An analytical absorption correction resulted in maximum and minimum transmission factors of 0.969 and 0.911, respectively. The structure was solved by direct methods<sup>14</sup> and expanded using Fourier techniques.<sup>15</sup> The non-hydrogen atoms were refined anisotropically. Hydrogen atoms were included in

idealized positions but not refined. The final cycle of full-matrix least-squares refinement on  $F^2$  was based on 2788 observed reflections and 280 variable parameters and converged (largest parameter shift was 0.00 times its esd) with unweighted and weighted agreement factors of  $R_1 = 0.039$  and  $wR_2 = 0.075$ . The standard deviation of an observation of unit weight was 1.63 (goodness fit factor). The weighting scheme was based on counting statistics and reflection order in data collection,  $\sin \theta/\lambda$  and various classes of indices showed no unusual trends. The maximum and minimum peaks on the final difference Fourier map corresponded to 0.31 and  $-0.28 \text{ e}^{-}/\text{Å}^3$  respectively. Neutral atom scattering factors were taken from Cromer and Waber.<sup>16</sup> Anomalous dispersion effects were included in  $F_{\text{calc}}$ .<sup>17</sup> All calculations were performed using the teXsan crystallographic software package of Molecular Structure Corporation.<sup>18</sup>

**X-ray Crystal Structure of  $[\text{LiC}12\text{-C-4}][\text{CF}_3\text{SO}_2\text{N}(\text{CH}_2)_3\text{OCH}_3]$  (II).** Crystals of  $[\text{LiC}12\text{-C-4}][\text{CF}_3\text{SO}_2\text{N}(\text{CH}_2)_3\text{OCH}_3]$  were grown by slow diffusion of diethyl ether into a solution of the complex in methylene chloride. A crystal with dimensions of  $0.42 \times 0.41 \times 0.29$  mm was mounted using oil (Paratone-N, Exxon) data collection and refinement follow those described for (I) and the crystallographic data is given in Table 1. The dimensions of the cell yield a calculated density of  $1.46 \text{ g cm}^{-3}$  ( $Z = 4$  and  $\text{FW} = 403.34$ ) and the systematic absence of  $h0l$ :  $l \pm 2n$  and  $0k0$ :  $k \pm 2n$  uniquely determines the space group to be  $P2_1/c$  (no. 14). The data were collected at a temperature of  $-120 \pm 1$  °C to a maximum  $2\theta$  value of  $56.7^\circ$ .

Of the 11 922 reflections collected, 4499 were unique ( $R_{\text{int}} = 0.013$ ). Data were collected and processed using the SMART (NT) and SAINT (NT) program (Bruker). A linear absorption coefficient,  $\mu$ ,  $2.4 \text{ cm}^{-1}$ , for Mo K $\alpha$  radiation was used. The data were corrected for Lorentz and polarization effects. A correction for secondary extinction was applied (coefficient =  $4.2686 \text{ e}^{-007}$ ). An empirical absorption correction was applied (SAD-ABS). An analytical absorption correction resulted in maximum and minimum transmission factors of 0.950 046 and 0.760 503, respectively.

The structure was solved as described for I. The final cycle of full-matrix least-squares refinement on  $F^2$  was based on 3492 observed reflections and 236 variable parameters and converged (largest parameter shift was 0.00 times its esd) with unweighted and weighted agreement factors of  $R_1 = 0.032$  and  $wR_2 = 0.060$ . The standard deviation of an observation of unit weight was 2.82 (goodness fit factor). The weighting scheme was based on counting statistics and reflection order in data collection,  $\sin \theta/\lambda$  and various classes of indices showed no unusual trends. The maximum and minimum peaks on the final difference Fourier map corresponded to 0.34 and  $-0.27 \text{ e}^{-}/\text{Å}^3$  respectively.

## Results and Discussion

**$(\text{Li}[\text{CF}_3\text{SO}_2\text{N}(\text{CH}_2)_3\text{OCH}_3])_2 \cdot \text{CH}_3\text{CN}$ .** Single-crystal X-ray diffraction reveals that the structure of  $(\text{Li}[\text{CF}_3\text{SO}_2\text{N}(\text{CH}_2)_3\text{OCH}_3])_2 \cdot \text{CH}_3\text{CN}$  consists of novel one-dimensional arrays of interconnected eight member puckered rings (Figure 1). The acetonitrile solvent molecules reside in alternate voids between the one-dimensional chains with the methyl groups approaching the chains, and the nitrogen atoms approximately stacked above each other. Figure 1 illustrates the connectivity in the one-dimensional array for five of the eight member rings. The lithium cation connects with the nitrogen atom, the sulfur atom, and sulfonyl oxygens. Eight member puckered rings include alternating

(13) Lascaud, S.; Perrier, M.; Vallee, A.; Besner, S.; Prud'homme, J.; Armand, M. *Macromolecules* **1994**, *27*, 7469.

(14) Altomare, A.; Cascarano, M.; Giacovazzo, C.; Guagliardi, A. *J. Appl. Crystallogr.* **1993**, *26*, 343.

(15) Beurskens, P. T.; Admiraal, G.; Beurskens, G.; Bosman, W. P.; Gelder, R. D.; Israel, R.; Smits, J. M. M. *The DIRDIF-94 Program System*; Technical Report of the Crystallography Laboratory: University of Nijmegen, 1994.

(16) Cromer, D. T.; Waber, J. T. *International Tables for X-ray Crystallography*; The Kynoch Press: Birmingham, 1974; Vol. IV.

(17) Ibers, J. A.; Hamilton, W. C. *Acta Crystallogr.* **1964**, *17*, 781.

(18) *Texsan for Windows 1.05: Crystal Structure Analysis Package*; Molecular Structure Corporation: The Woodlands, TX, 1997.

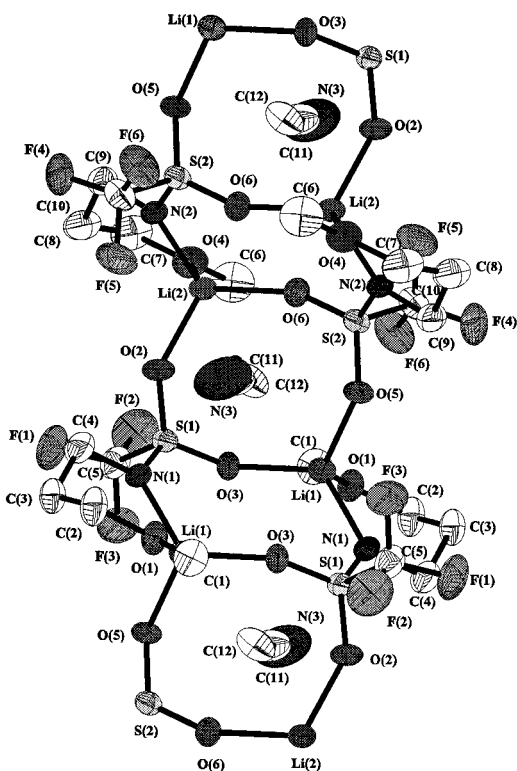


**Figure 1.** A five ring section of the packing diagram of  $\text{Li}[\text{CF}_3\text{SO}_2\text{N}(\text{CH}_2)_3\text{OCH}_3]_2 \cdot \text{CH}_3\text{CN}$  down the  $b$  axis. Thermal ellipsoids are at 50% probability.

rings: (a) Li(1), N(1), S(1), and O(3) (ring has a center of inversion); (b) S(1), O(2), Li(2), O(6), S(2), O(5), Li(1), and O(3)—from the perspective in Figure 1 an acetonitrile molecule, which is noncoordinating, appears to reside in the ring (the view is down the  $b$  axis) but it actually resides between ring layers); and (c) Li(2), N(2), S(2) and O(6) (ring has a center of inversion). Rings with centers of inversion are capped at both ends with the remaining  $[\text{CF}_3\text{SO}_2\text{N}(\text{CH}_2)_3\text{OCH}_3]^-$  anions forming six member rings such as Li(2), O(4), C(7), C(8), C(9), and N(2) and Li(1), O(1), C(2), C(3), C(4), and N(1).

The coordination environment of the lithium cation in  $\text{Li}[\text{CF}_3\text{SO}_2\text{N}(\text{CH}_2)_3\text{OCH}_3]$  is unlike that of the related lithium salts,  $\text{Li}[\text{CF}_3\text{SO}_2\text{N}-\text{R}]$ , where R is not an alkoxy group.<sup>19–22</sup> In those salts the lithium cation typically coordinates to the oxygens of the S–O group and the nitrogen. In the present structure the ether oxygen, sulfonyl oxygen and nitrogen atom in  $[\text{CF}_3\text{SO}_2\text{N}(\text{CH}_2)_3\text{OCH}_3]^-$  coordinates to the lithium. Figure 2 illustrates the four-coordinate environment of the lithium cation which is composed of the nitrogen and an ether oxygen of one anion, and a sulfonyl oxygen from each of two different anions. The flexibility imparted by the ether oxygen in the anion may contribute to the substantial conductivity in these electrolytes.

The bond distances observed in  $\text{Li}[\text{CF}_3\text{SO}_2\text{N}(\text{CH}_2)_3\text{OCH}_3]$  (Table 2) are comparable to those in an analogous salt,  $\text{Li}[(\text{CF}_3\text{SO}_2)_2\text{N}]$ .<sup>19</sup> The coordination environ-

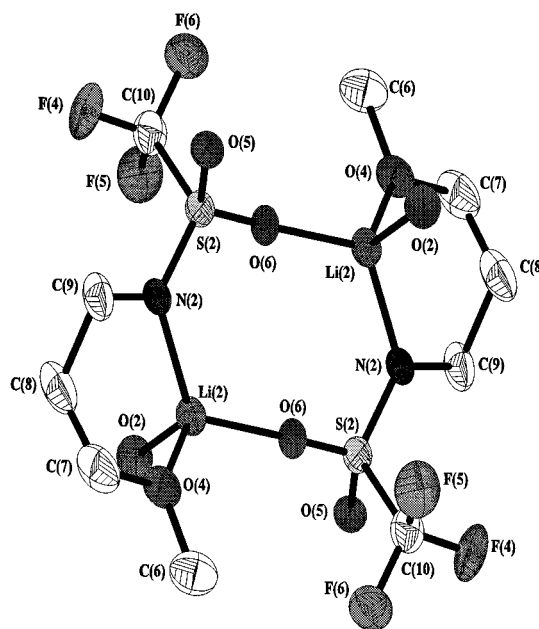


**Figure 2.** Coordination environment of the lithium cation in  $\text{Li}[\text{CF}_3\text{SO}_2\text{N}(\text{CH}_2)_3\text{OCH}_3]_2 \cdot \text{CH}_3\text{CN}$ . Thermal ellipsoids are at 50% probability.

ments around the respective lithium cations are not the same but lithium coordinates to sulfonyl oxygens in both structures and both anions contain the  $-\text{NSO}_2\text{CF}_3$  group. The negative charge on  $[(\text{CF}_3\text{SO}_2)_2\text{N}]^-$  is believed to be delocalized over the S–N and S–O bonds. The S–N bond distance in  $\text{Li}[(\text{CF}_3\text{SO}_2)_2\text{N}]$  is  $\sim 1.557 \text{ \AA}$ , which reflects partial double-bond character, whereas the S–N bond in  $\text{Li}[\text{CF}_3\text{SO}_2\text{N}(\text{CH}_2)_3\text{OCH}_3]$ ,  $1.517 \text{ \AA}$ , is shorter indicating substantial double bond character. In  $\text{Li}[\text{CF}_3\text{SO}_2\text{N}(\text{CH}_2)_3\text{OCH}_3]$ , the negative charge of the anion is delocalized over a single S–N bond ( $\text{Li}[(\text{CF}_3\text{SO}_2)_2\text{N}]$  has two S–N bonds). The trend in bond distances does not extend to that of S–O in  $\text{Li}[\text{CF}_3\text{SO}_2\text{N}(\text{CH}_2)_3\text{OCH}_3]$  where the S–O distance might be expected to be longer. In fact, there are small differences between the S–O bond distances of  $\text{Li}[\text{CF}_3\text{SO}_2\text{N}(\text{CH}_2)_3\text{OCH}_3]$ ,  $1.442$ – $1.451 \text{ \AA}$ , and  $\text{Li}[(\text{CF}_3\text{SO}_2)_2\text{N}]$ ,  $1.429$ – $1.451 \text{ \AA}$ . This observation supports the assertion of Golding et al. that charge delocalization may occur on the S–N bond and not on the S–O as previously postulated.<sup>23</sup>

An interesting feature of the  $\text{Li}[\text{CF}_3\text{SO}_2\text{N}(\text{CH}_2)_3\text{OCH}_3]$  structure is the variation of bond distances between the lithium cation and its respective coordinating groups. The Li–N bond,  $1.997 \text{ \AA}$ , is the longest interaction followed closely by  $1.943 \text{ \AA}$  for Li(2)–O(4) (ether oxygen). The shortest bond distances occur between lithium and sulfonyl oxygens (Li–O ( $1.915 \text{ \AA}$ ) and Li–O ( $1.918 \text{ \AA}$ )). These bond distances and bond angles around the lithium cation will be the focus for the comparison with  $[\text{Li}-12-\text{C}-4][\text{CF}_3\text{SO}_2\text{N}(\text{CH}_2)_3\text{OCH}_3]$ .

Previous infrared data for  $\text{Li}[\text{CF}_3\text{SO}_2\text{N}(\text{CH}_2)_3\text{OCH}_3]$  indicated coordination of the lithium cation to the ether oxygen of the anion,  $[\text{CF}_3\text{SO}_2\text{N}(\text{CH}_2)_3\text{OCH}_3]^-$ .<sup>12</sup> Simple aliphatic ethers absorb near  $1125 \text{ cm}^{-1}$  as a single strong asymmetric C–O–C stretching band ( $\nu_{\text{as}} \text{ C-O-C}$ ). However, small cyclic ether linkages exhibit  $\nu_{\text{as}}$

(19) Nowinski, J. L.; Lightfoot, P.; Bruce, P. G. *J. Mater. Chem.* **1994**, *4*, 1579.

(20) Haas, A.; Klare, C.; Betz, P.; Bruckmann, J.; Kruger, C.; Tsay, Y.-H.; Aubke, F. *Inorg. Chem.* **1996**, *35*, 1918.

(21) Zak, Z.; Ruzicka, A. *Z. Kristallogr.* **1998**, *213*, 217.

(22) Xue, L.; DesMarteau, D. D.; Pennington, W. T. *Angew. Chem. Int. Ed. Engl.* **1997**, *26*, 11331.

(23) Golding, J. J.; MacFarlane, D. R.; Spiccia, L.; Forsyth, M.; Skelton, B. W.; White, A. H. *Chem. Commun.* **1998**, 1593.



**Table 2. Selected Bond Lengths (Å) and Bond Angles (deg) for  $(\text{Li}[\text{CF}_3\text{SO}_2\text{N}(\text{CH}_2)_3\text{OCH}_3])_2 \cdot \text{CH}_3\text{CN}$** 

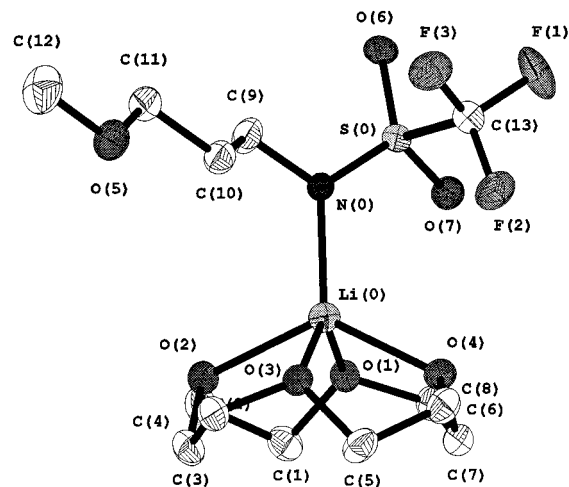
atom	atom	distance	atom	atom	distance
S1	O2	1.451(2)	S1	O3	1.442(2)
S1	N1	1.517(3)	S1	C5	1.832(4)
S2	O5	1.449(2)	S2	O6	1.448(2)
S2	N2	1.520(3)	S2	C10	1.839(4)
F1	C5	1.331(4)	F2	C5	1.326(4)
F3	C5	1.317(4)	F4	C10	1.318(4)
F5	C10	1.333(4)	F6	C10	1.335(4)
O1	C1	1.425(4)	O1	C2	1.425(4)
O1	LI1	1.942(6)	O2	LI2	1.919(6)
O3	LI1	1.915(6)	O4	C6	1.427(4)
O4	C7	1.421(4)	O4	LI2	1.943(6)
O5	LI1	1.918(6)	O6	LI2	1.918(6)
N1	C4	1.489(4)	N1	LI1	1.990(6)
N2	C9	1.480(4)	N2	LI2	1.997(6)
N3	C11	1.117(5)	C1	H1	0.95

atom	atom	atom	angle	atom	atom	atom	angle
O2	S1	O3	116.6(1)	S2	N2	LI2	121.5(2)
O2	S1	N1	116.3(1)	C9	N2	LI2	119.4(3)
O2	S1	C5	101.3(2)	O1	C2	C3	110.5(3)
O3	S1	N1	111.1(1)	C2	C3	C4	115.8(3)
O3	S1	C5	100.6(2)	N1	C4	C3	109.8(3)
N1	S1	C5	108.9(2)	S1	C5	F1	110.7(3)
O5	S2	O6	116.3(1)	S1	C5	F2	112.0(3)
O5	S2	N2	116.2(1)	S1	C5	F3	111.4(3)
O5	S2	C10	101.2(2)	F1	C5	F2	107.7(3)
O6	S2	N2	111.2(1)	F1	C5	F3	107.4(3)
O6	S2	C10	100.9(2)	F2	C5	F3	107.4(3)
N2	S2	C10	109.1(2)	O4	C7	C8	110.5(3)
C1	O1	C2	112.3(3)	C7	C8	C9	116.4(3)
C1	O1	LI1	123.9(3)	N2	C9	C8	110.0(3)
C2	O1	LI1	123.7(3)	S2	C10	F4	111.7(3)
S1	O2	LI2	145.4(2)	S2	C10	F5	110.7(3)
S1	O3	LI1	152.3(2)	S2	C10	F6	111.1(2)
C6	O4	C7	112.2(3)	F4	C10	F5	108.0(3)
C6	O4	LI2	122.9(3)	F4	C10	F6	108.0(3)
C7	O4	LI2	123.6(3)	F5	C10	F6	107.1(3)
S2	O5	LI1	145.0(2)	N3	C11	C12	179.4(5)
S2	O6	LI2	152.9(2)	O1	LI1	O3	103.7(3)
S1	N1	C4	118.2(2)	O1	LI1	O5	112.1(3)
S1	N1	LI1	121.7(2)	O1	LI1	N1	95.0(3)
C4	N1	LI1	120.0(3)	O3	LI1	O5	111.8(3)
S2	N2	C9	117.8(2)	O3	LI1	N1	121.7(3)
O5	LI1	N1	110.8(3)	O4	LI2	O6	104.3(3)
O2	LI2	O4	108.5(3)	O4	LI2	N2	93.9(2)
O2	LI2	O6	114.5(3)	O6	LI2	N2	119.2(3)
O2	LI2	N2	113.2(3)				

C–O–C bands at lower wavenumbers.<sup>24</sup> Infrared bands at 1091 and 1106  $\text{cm}^{-1}$  for  $\text{Li}[\text{CF}_3\text{SO}_2\text{N}(\text{CH}_2)_3\text{OCH}_3]$  infrared bands at 1091 and 1106  $\text{cm}^{-1}$  are assigned as  $\nu_{\text{as}}$  C–O–C. The low frequency of both bands suggests that the ether oxygen is part of a small ring arrangement.

**$[\text{Li}12\text{-C-4}][\text{CF}_3\text{SO}_2\text{N}(\text{CH}_2)_3\text{OCH}_3]$ .** The coordination in  $[\text{Li}12\text{-C-4}][\text{CF}_3\text{SO}_2\text{N}(\text{CH}_2)_3\text{OCH}_3]$  is similar to that of other  $\text{Li}12\text{-C-4}$  complexes.<sup>25–27</sup> The lithium cation is coordinated to four ether oxygens of the 12-C-4 macrocycle and the nitrogen atom of the anion. A striking feature in the structure of  $[\text{Li}12\text{-C-4}][\text{CF}_3\text{SO}_2\text{N}(\text{CH}_2)_3\text{OCH}_3]$  is the absence of lithium coordination to the ether and sulfonyl oxygens of the anion. The

**Figure 3.** Coordination environment of the lithium cation in  $[\text{Li}12\text{-C-4}][\text{CF}_3\text{SO}_2\text{N}(\text{CH}_2)_3\text{OCH}_3]$ . Thermal ellipsoids are at 50% probability.

lithium atom is five-coordinate with an approximate square-pyramidal geometry consisting of four basal oxygen atoms and an apical nitrogen atom (Figure 3). The Li–N bond distance is long, 2.011 Å, and this is attributed to the macrocycle pulling the lithium cation away from the anion. The long Li–N bond confirms that the 12-C-4 macrocycle reduces the strength of the ion pairing.

The disposition of the ether oxygens is exceptionally uniform as indicated by the small mean deviation from a plane of the ether oxygens, 0.0149 Å. The lithium cation resides 0.912 Å above the plane of the crown ether oxygens in  $[\text{Li}12\text{-C-4}][\text{CF}_3\text{SO}_2\text{N}(\text{CH}_2)_3\text{OCH}_3]$ . This distortion is greater than that of a lithium 12-C-4 complexes but a rationale for this difference is not evident.<sup>28</sup> The lithium–crown bond distances are grouped into two long bonds (2.187 and 2.164 Å) and two shorter bonds (2.080 and 2.086 Å). Longer Li–O distances are typically observed in octahedral complexes relative to tetrahedral complexes. The Li–O (crown) bond distance in  $[\text{Li}12\text{-C-4}][\text{CF}_3\text{SO}_2\text{N}(\text{CH}_2)_3\text{OCH}_3]$  is within the range of those observed in analogous complexes.<sup>29,30</sup>

$\text{Li}[\text{CF}_3\text{SO}_2\text{N}(\text{CH}_2)_3\text{OCH}_3]$  has a very short S–N bond distance (1.517 Å) which lengthens slightly, 1.534 Å, upon coordination to 12-C-4, indicating decreased delocalization over the S–N bond (Table 3). The S–O bond distances in  $\text{Li}[\text{CF}_3\text{SO}_2\text{N}(\text{CH}_2)_3\text{OCH}_3]$ , 1.451 and 1.442 Å, are similar to those in  $[\text{Li}12\text{-C-4}][\text{CF}_3\text{SO}_2\text{N}(\text{CH}_2)_3\text{OCH}_3]$ , 1.4468 and 1.4407 Å, indicating the high sensitivity of the S–N bond to changes in the coordination environment.

The coordination of lithium in  $\text{Li}[\text{CF}_3\text{SO}_2\text{N}(\text{CH}_2)_3\text{OCH}_3]$  to the ether oxygen of the anion to form part of a six member ring is attributed to the small C(9)–N(2)–Li(2) bond angle, 119.4° (Table 3). The analogous C(9)–N(0)–Li(0) bond angle in  $[\text{Li}12\text{-C-4}][\text{CF}_3\text{SO}_2\text{N}(\text{CH}_2)_3\text{OCH}_3]$  is larger (124.1°) because the 12-C-4 macrocycle breaks the Li(2)–O(4) interaction and consequently the ring motif. This ring strain also explains the large bond

(24) Colthup, N. B.; Daly, L. H.; Wiberly, S. E. *Introduction to Infrared and Raman Spectroscopy*, 2 ed.; Academic Press: New York, 1975.

(25) Gingl, F.; Hiller, W.; Strahle, J. *Z. Anorg. Allg. Chem.* **1991**, 606, 91.

(26) Pauer, F.; Rocha, J.; Stalke, D. *J. Chem. Soc., Chem. Commun.* **1991**, 1477.

(27) Power, P. P.; Xiaojie, X. *J. Chem. Soc. Chem. Commun.* **1984**, 358.

(28) Shoham, G.; Lipscomb, W. N.; Olsher, U. *J. Chem. Soc. Chem. Commun.* **1983**, 208.

(29) Bartlett, R. A.; Power, P. P. *J. Am. Chem. Soc.* **1987**, 109, 6509.

(30) Chen, H.; Bartlett, R. A.; Dias, H. V. R.; Olmstead, M. M.; Power, P. P. *J. Am. Chem. Soc.* **1989**, 111, 4338.

**Table 3. Selected Bond Lengths (Å) and Bond Angles (deg) for [Li-12-C-4][CF<sub>3</sub>SO<sub>2</sub>N(CH<sub>2</sub>)<sub>3</sub>OCH<sub>3</sub>]**

atom	atom	distance	atom	atom	distance
S	O6	1.4468(11)	S	O7	1.4407(11)
S	N	1.5338(13)	O1	C1	1.432(2)
O1	C8	1.435(2)	O1	LI	2.086(3)
O2	C2	1.435(2)	O2	C3	1.438(2)
O2	LI	2.164(3)	O3	C4	1.435(2)
O3	C5	1.436(2)	O3	LI	2.187(3)
O4	C6	1.433(2)	O4	C7	1.433(2)
O4	LI	2.080(3)	O5	C11	1.418(2)
O5	C12	1.423(2)	N	C9	1.476(2)
N	LI	2.011(3)	C1	C2	1.508(2)

atom	atom	atom	angle	atom	atom	atom	angle
O6	S	O7	117.57(7)	O6	S	N	115.91(7)
O6	S	C13	101.03(7)	O7	S	N	111.71(7)
O7	S	C13	101.35(7)	N	S	C13	106.83(7)
C5	O3	LI	108.33(12)	C3	O2	LI	111.02(12)
O3	LI	N	115.37(13)	C4	O3	LI	110.51(12)
C6	O4	LI	111.03(12)	C7	O4	LI	109.67(12)
C11	O5	C12	111.6(1)	S	N	C9	118.05(10)
S	N	LI	117.70(11)	C9	N	LI	124.10(13)
C7	C8	H16	109.1	H15	C8	H16	109.5
N	C9	C10	112.51(13)	N	C9	H17	108.7
N	C9	H18	108.7	C10	C9	H17	108.7
C10	C9	H18	108.7	H17	C9	H18	109.5
C9	C10	C11	112.5(1)	C9	C10	H19	108.7
O1	LI	O2	79.28(10)	O1	LI	O3	128.42(13)
O1	LI	O4	81.73(11)	O1	LI	N	116.08(13)
O2	LI	O3	77.32(10)	O2	LI	O4	129.82(13)
O2	LI	N	113.73(13)	O3	LI	O4	79.22(10)
O4	LI	N	116.4(1)				

angle of C(7)–C(8)–C(9), 116.43°, in Li[CF<sub>3</sub>SO<sub>2</sub>N(CH<sub>2</sub>)<sub>3</sub>OCH<sub>3</sub>]. Therefore, it is not surprising that a more normal bond angle is observed, C(9)–C(10)–C(11), 112.5°, in [Li-12-C-4][CF<sub>3</sub>SO<sub>2</sub>N(CH<sub>2</sub>)<sub>3</sub>OCH<sub>3</sub>]. The bond

angle S(2)–N(2)–Li(2), 121.5°, in Li[CF<sub>3</sub>SO<sub>2</sub>N(CH<sub>2</sub>)<sub>3</sub>OCH<sub>3</sub>] is part of a larger eight member ring.

Raman spectra of [Li-12-C-4][CF<sub>3</sub>SO<sub>2</sub>N(CH<sub>2</sub>)<sub>3</sub>OCH<sub>3</sub>] contain a band at 863 cm<sup>-1</sup> assigned as a symmetric ring breathing motion of 12-C-4 crown ether oxygens surrounding solvated cations.<sup>31</sup> Infrared spectra of this complex indicate significant changes in S–O stretching frequencies relative to Li[CF<sub>3</sub>SO<sub>2</sub>N(CH<sub>2</sub>)<sub>3</sub>OCH<sub>3</sub>], in keeping with the difference in structures.

## Conclusions

The structure of Li[CF<sub>3</sub>SO<sub>2</sub>N(CH<sub>2</sub>)<sub>3</sub>OCH<sub>3</sub>] is unusual for salts containing the CF<sub>3</sub>SO<sub>2</sub>N moiety because lithium coordinates to the ether oxygen in the anion as well as the nitrogen and sulfonyl oxygens. The anion is slightly bent to facilitate ether oxygen coordination to the lithium cation. Also, the 12-C-4 macrocycle draws the lithium cation away from the ether oxygen and sulfonyl oxygen of the anion. In this process, the lithium adopts a square-pyramidal coordination with four ether oxygens of the crown ether and the nitrogen atom of the anion. This environment is likely to facilitate ionic conductivity. The flexibility of the ether oxygen in the anion may promote ion motion.

**Acknowledgment.** This research was supported by the MRSEC program of the National Science Foundation (DMR-9632472) at the Materials Research Center of Northwestern University.

(31) Sato, H.; Kusumoto, Y. *Chem. Lett.* **1978**, 635.